Essential Readings in Light Metals: Electrode Technology for Aluminum Production.
Edited by Alan Tomsett and John Johnson.

Light Metals — From ***Light Metals 1995***, James W. Evans, Editor

PROPERTY CHANGES OF CATHODE LINING MATERIALS DURING CELL OPERATION

Morten Sørlie and **Hermann Gran**
Elkem a/s Research
P.O.Box 40 Vågsbygd
N-4602 KRISTIANSAND, Norway

Harald A. Øye
Institute of Inorganic Chemistry
The Norwegian Institute of Technology
N-7034 TRONDHEIM, Norway

ABSTRACT

Carbon cathode materials are catalytically graphitized during the aluminium electrolysis. The graphitization has been characterized by X-ray diffraction. The graphitization and salt penetration cause profound changes in electrical and thermal conductivities. These properties have been determined for different commercial cathode materials as function of operational time and temperature. The assumed correlation between electrical and thermal conductivity is found to be poor. The changes in thermal conductivities of refractory and insulation materials have also been determined and actual examples of cell deterioration are given. Heat balance calculations based on the changing values of electrical and thermal conductivities demonstrate drastic changes as the cell get older. Calculations based only on virgin materials properties will give quite erroneous results.

INTRODUCTION

In traditional designs of industrial aluminium electrolysis cells the cathode bottoms are lined with prebaked carbon blocks that act as electrical current conductors as well as a refractory lining that serves as a container for the fused cryolite electrolyte and the liquid aluminium pool. The blocks are normally made from calcined anthracite, graphite or a combination of these materials [1]. The amount of inorganic impurities are typically 4-8 % in fully anthracitic blocks and <0.5 % in graphitic blocks.

At normal electrolysis temperatures the bottom blocks become impregnated with sodium metal and bath constituents. These migrating species will participate in a number of chemical reactions with carbon block impurities and gas species already present in the porosity or migrating the opposite way [2-4]. Eventually the electrolyte species and their reaction products will fill all the available open porosity of the cathode block. The ash content of used carbon blocks, *i.e.* the inorganic matter remaining after removal of all carbon by air oxidation, may reach 40 %.

Bath components that percolate through the bottom carbon lining will reach the oxide refractories underneath and will, depending on their chemical composition, react chemically to a greater or lesser extent with these [5-8].

The temperature of electrolysis is not high enough for a thermal graphitization of carbon to take place. This is particularly true with amorphous blocks made from anthracite which is a hard carbon and normally will need temperatures close to or above 2000°C in order to show any significant degree of graphitization.*

However, the cell operating temperature is sufficiently high for a catalytic graphitization of the carbon lining to take place. Amorphous bottom blocks made from calcined anthracite and a coal tar pitch binder becomes partially graphitized during operation. It has been shown [9] that within about one year in service, there were practically no measurable differences in electrical resistivity between cathode blocks made with a dry aggregate of 100 % anthracite and blocks made with considerable amounts of graphite in the dry aggregate.

The paper discusses the changes in electrical properties, thermal properties and structure of carbon and oxide lining materials as a function of the service life. The effect such changes may have on industrial electrolysis cells are also discussed.

EXPERIMENTAL

Bottom block samples were taken from new bottom blocks and from failed cathodes at the Elkem Aluminium Lista and Elkem Aluminium Mosjøen smelters in Norway. A qualitative description of the various bottom block qualities are listed in Table 1. Capital letters A-D denote different producers. The number behind the producer identification letter (1-5) is a code for block quality (composition), *i.e.* the same number corresponds roughly to similar (comparable) quality. The fully graphitized blocks (C5,D5) have been heat treated close to 3000°C and are included for reference purposes only. Both filler and binder in these are fully graphitized. Reference [1] should be consulted for a more thorough description of the classification of bottom blocks.

All samples of failed cathodes were from the middle part of the cathode bottom pane (blocks) with a minimum distance to any side or end of 1/4 of the cathode width or length, respectively. Electrical resistivity and thermal conductivity were measured on cores drilled perpendicular to the cathode surface. Electrical resistivity was measured from room temperature to 1000°C while the maximum temperature for the thermal conductivity measurements was 700°C.

* Gas calcined anthracite (GCA) is a 100 % amorphous material while electro calcined anthracite (ECA) will contain some partially graphitized material due to local very high temperatures during calcination [1].

Table 1. Types of cathode blocks.

Block	Type	Dry aggregate
A1	Amorphous	ECA
A2	Amorphous	ECA + G (minor amounts)
A3	Amorphous	ECA + G (considerable amounts)
A4	Semigraphitic	G
B2	Amorphous	ECA + G (minor amounts)
B3	Amorphous	ECA + G (considerable amounts)
B4	Semigraphitic	G
C5	Graphitized	
D5	Graphitized	

ECA: electro calcined anthracite
G: synthetic graphite

The experimental set-up to perform the electrical and thermal measurements at elevated temperatures as well as the experimental procedures have been described elsewhere [10,11].

The degree of graphitization was measured by two different methods based on X-ray powder diffraction. One method uses the interlayer distance (d_{002}) to calculate the degree of graphitization [12] while the other one is a relative method based on the intensity ratio of the 002 diffraction peak of the spent cathode carbon relative to a defined graphite standard [13]. The fluoride salts that filled the carbon porosity were, in order to avoid interference, removed by boiling the crushed samples in an aqueous $AlCl_3$ solution prior to the X-ray diffraction measurements.

Samples of used and chemically converted refractory materials were also taken from autopsied pots and analyzed.

RESULTS AND DISCUSSION

Carbon. Figure 1 and Figure 2 show how the electrical resistivity of a range of different bottom blocks from two producers (A,B), ranging from pure electro-calcined anthracite (ECA) to semi-graphitic grades, vary with temperature. Block C5 on Figure 2 is fully graphitized and included for comparison. It is seen that electrical resistivities of the semi-graphitic qualities A4 and B4, *i.e.* graphitic aggregate but non-graphitized binder coke (baked to normal baking temperatures, 1050°C-1200°C) are comparable, while more amorphous grades are not.

Thermal conductivity *versus* temperature measured on the same virgin cathode blocks are given in Figure 3 and Figure 4. Block D5 on Figure 4 is fully graphitized and included for comparison. The thermal conductivities for the "similar" amorphous qualities A2 and B2 are comparable while the two semi-graphitic qualities A4 and B4 differ significantly. Although almost comparable at room temperature the A4 semi-graphitic material increases its thermal conductivity as the temperature is increased and follows in this respect the qualitative development of the more amorphous blocks. The B4 block, on the other hand, shows a temperature development more in line with what is expected in graphitized or partly graphitized materials, *i.e.* the thermal conductivity drops as the temperature is increased.

When thermal shock resistance of cathode bottom blocks are calculated the thermal conductivity value is used in the nominator of the standard expression. Since the room temperature electrical resistivity normally is simpler to measure, and often considered inversely proportional to the thermal conductivity of the material,

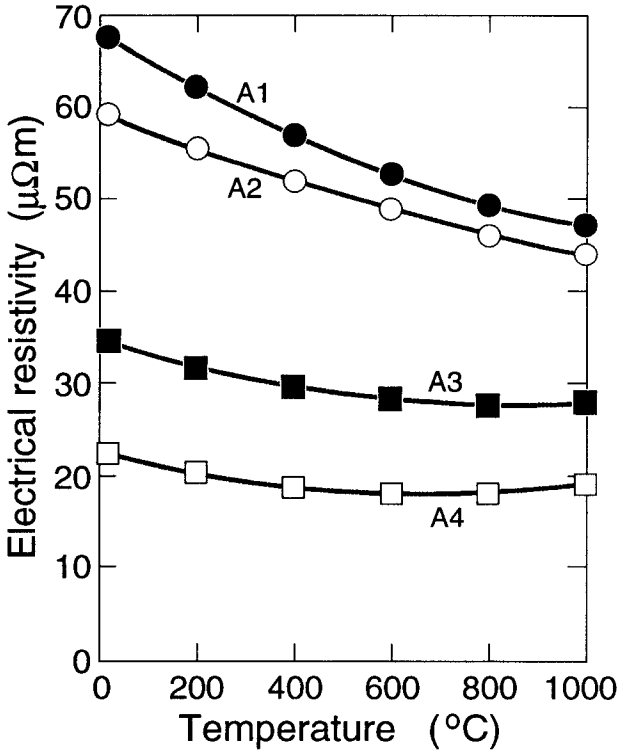

Figure 1. Electrical resistivity of virgin cathode bottom blocks from producer A for the temperature range up to 1000°C.

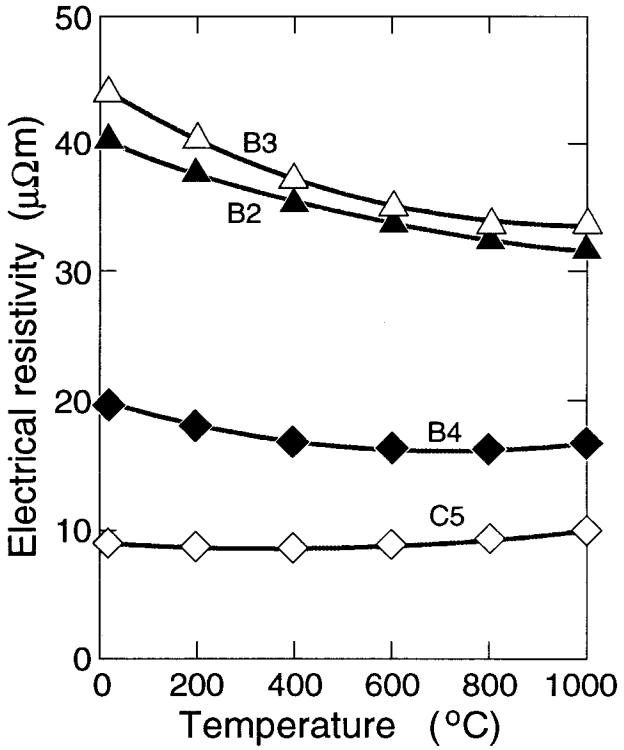

Figure 2. Electrical resistivity of virgin cathode bottom blocks from producer B for the temperature range up to 1000°C. Block C5 (fully graphitized) is included for comparison.

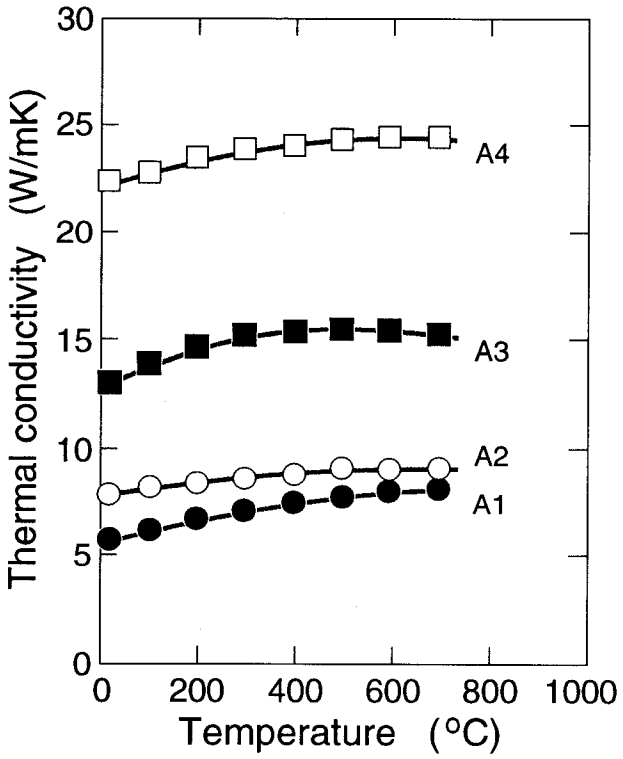

Figure 3. Thermal conductivity of virgin cathode bottom blocks from producer A for the temperature range up to 700°C.

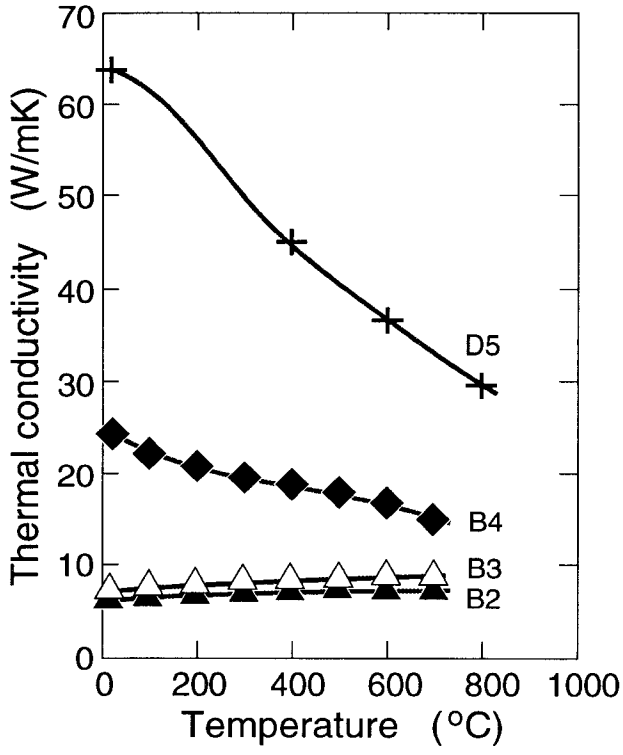

Figure 4. Thermal conductivity of virgin cathode bottom blocks from producer B for the temperature range up to 700°C. Block D5 (fully graphitized) is included for comparison.

the electrical properties are sometimes used in the denominator of the same expression. This can be a questionable practice since Figures 1-4 show that there is no general proportionality between these properties.

During cell operation the amorphous bottom block material experiences a structural rearrangement to a more graphitic carbon at normal cell operating temperatures [9]. This have a pronounced effect on the electrical resistivity (Figure 5 and Figure 6) as well as thermal conductivity (Figure 7 and Figure 8) of the bottom blocks, which in old cathodes can attain values of fairly well graphitized materials. A 7.2 year old block of type B3 has obtained a higher thermal conductivity (Figure 8) than the virgin graphitized block D5 (Figure 4). Its electrical resistivity (Figure 6), however, does not quite match the electrical resistivity of the graphitized block C5 (Figure 2).

There is a considerable scatter for the values of thermal and electrical properties of used cathode blocks *versus* age (Figure 9 and Figure 10). The properties are given for two temperatures. The figures include bottom block types and producers not listed in Table 1 but all are amorphous block qualities with 0-30 % synthetic graphite added. Virgin materials are not included in the figures. The electrical and thermal properties of a certain type of bottom block or amorphous blocks in general do not reach entirely uniform levels with time. Although definite trends are evident, the change in properties with age can better be described by a rather broad band that give room for considerable scatter. The reasons for this can be several: Different producers may use raw materials from different sources and may even juggle raw materials for a given quality or type of bottom block. The exposure to sodium and bath may also be different.

There is also poor correlation between thermal and electrical properties and caution should again be exercised in assuming one of the properties from the other. In Figure 11 thermal conductivity and electrical resistivity values at 20°C and 500°C are plotted against each other for virgin as well as used cathode blocks.

The catalytic graphitization is attempted characterized by two methods (Table 2):

a) The degree of graphitization (g in %) defined by Maire and Méring [12]:

$$g = 100\frac{3.44 - d_{002}}{0.086} \qquad (1)$$

b) The d_{002} peak ratio (p_{002} in %) defined by Aune et al. [13]:

$$p_{002} = \frac{\frac{I_s}{m_s}}{\frac{I_r}{m_r}} 37 \qquad (2)$$

where $\frac{I}{m}$ is the X-ray intensity/mass ratio and subscripts s and r are unknown sample and reference, respectively. The reference is a CS-49B graphite.

The graphitization ratio g is a useful parameter for characterization of soft carbons above 1800°C. In most amorphous cathodes, however, synthetic graphite is mixed in so that the location of the d_{002} peak will always be very close to d_{002} for single crystal graphite. The g value hence gives completely unrealistic results as seen from Table 2.

The peak ratio appears to describe the graphitization in a very realistic and probable way. Synthetic graphite has p_{002} equal to 37 % [1]. The amount of synthetic graphite in the unused block B3 can then be calculated to: (9.7/37)·100 = 26 %. This value is very close

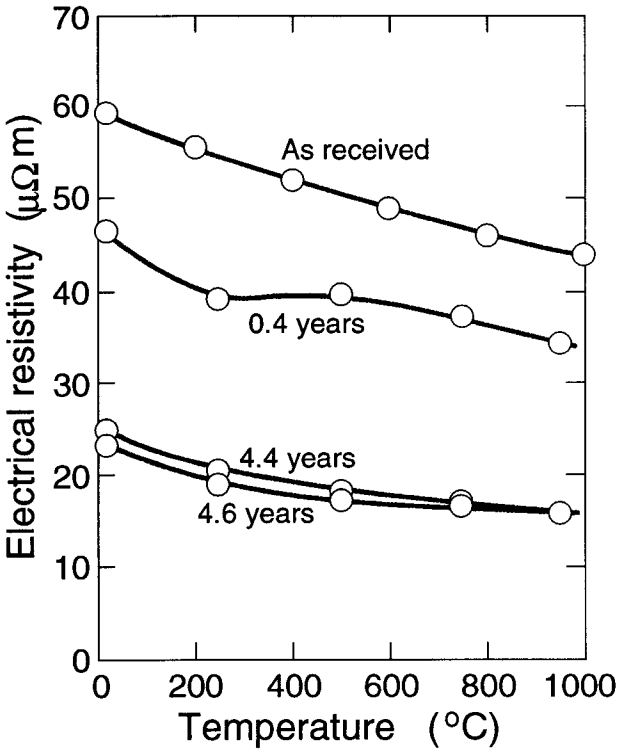

Figure 5. Electrical resistivity of used cathode bottom blocks of type A2 for the temperature range up to 1000°C.

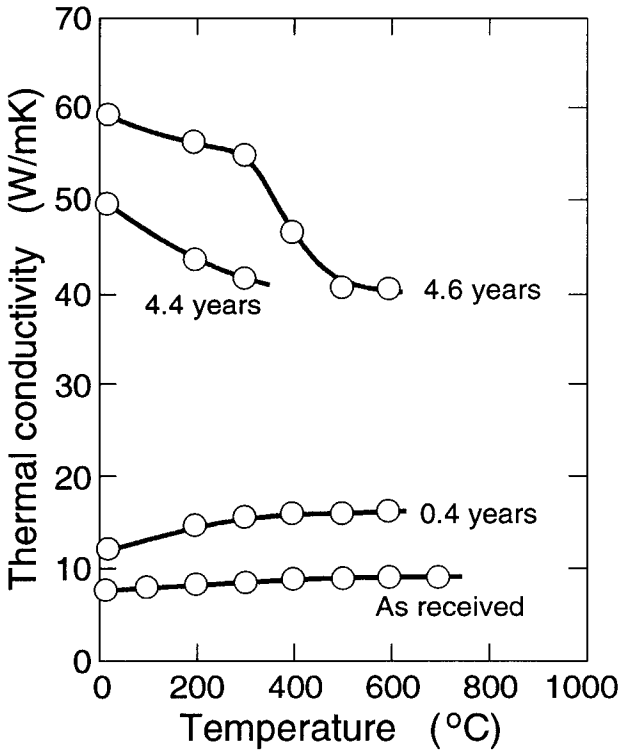

Figure 7. Thermal conductivity of used cathode bottom blocks of type A2 as function of temperature.

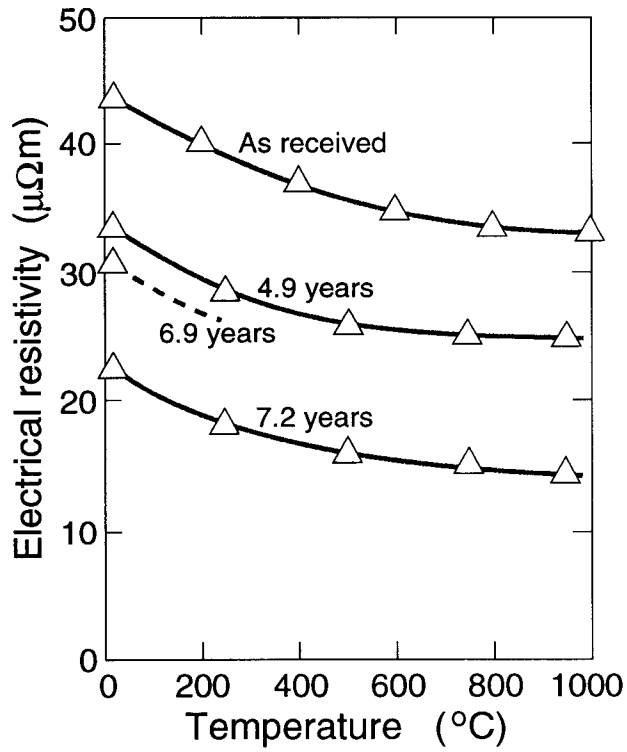

Figure 6. Electrical resistivity of used cathode bottom blocks of type B3 for the temperature range up to 1000°C.

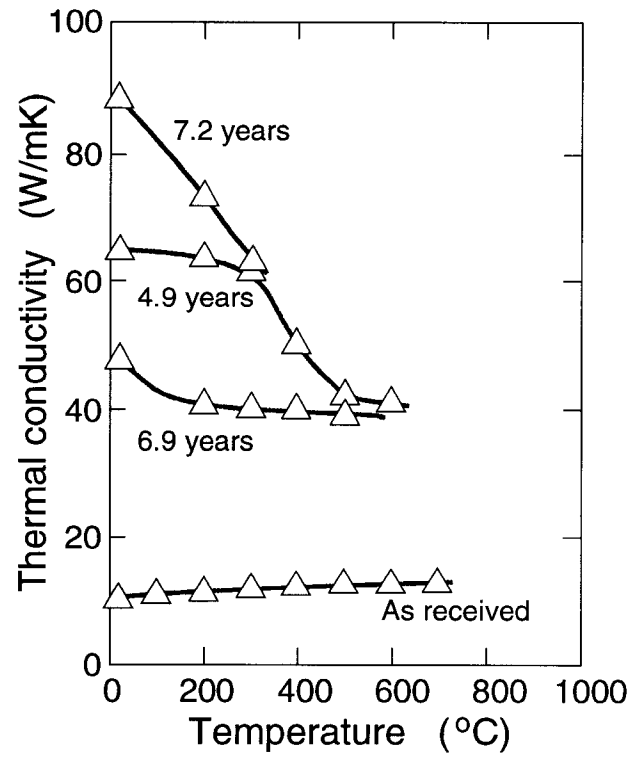

Figure 8. Thermal conductivity of used cathode bottom blocks of type B3 as function of temperature.

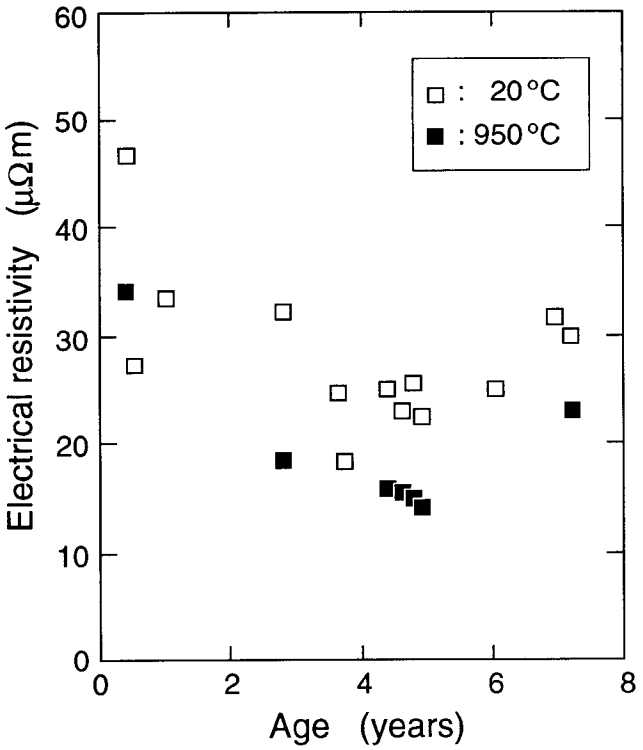

Figure 9. Electrical resistivity of amorphous bottom blocks as a function of service life in industrial cells.

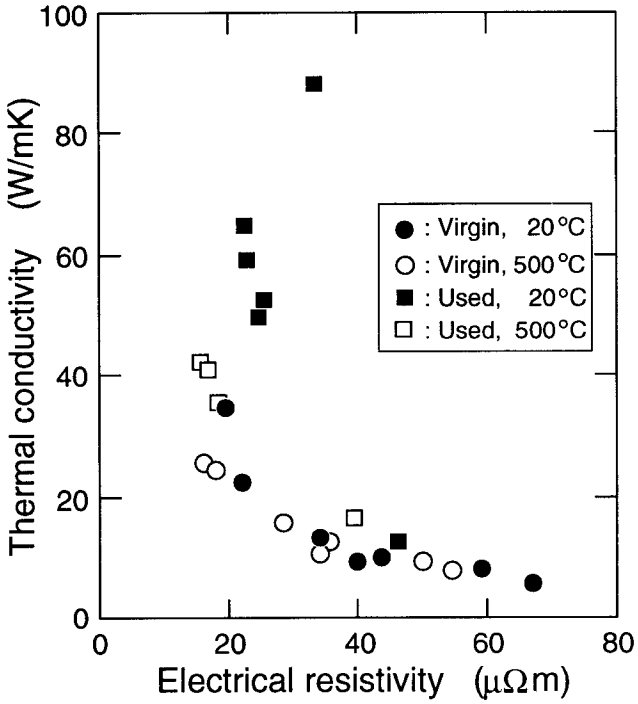

Figure 11. Correlation between measured (20°C and 500°C) thermal and electrical properties of virgin and used cathode blocks.

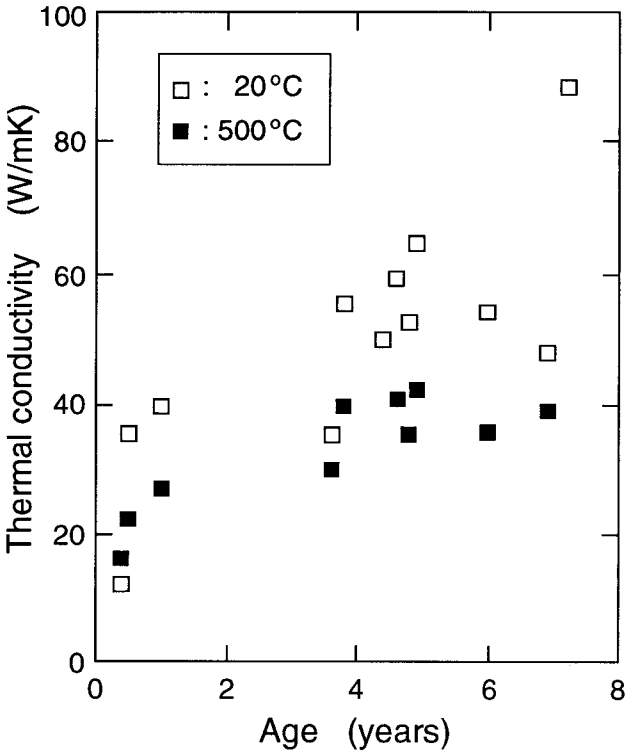

Figure 10. Thermal conductivity of amorphous bottom blocks as a function of service life in industrial cells.

to the expected real amount of synthetic graphite mixed into the block. The amount of graphite based on the peak ratio is seen to increase steadily with service life for block B3 and is at 7.2 years equal to (32.1/37)·100 = 86 %. The peak ratio then confirm the belief that the catalytic graphitization process is slow. It appears, however, to be nearly complete within about 7 years. The measured electrical resistivities (Figure 6) and thermal conductivities (Figure 8) supports this description.

The structure of disordered carbons and their ease of graphitization depends on how they are formed. Soft, or graphitizing carbons, such as petroleum coke and pyrolytic carbon, are readily converted to graphite at a heat treatment temperature (HTT) of ≈2700°C. Hard, or non-graphitizing carbons, which often contain impurity atoms (O,N,H,S), such as glassy or cellulose carbons, are not completely converted to graphite even at temperatures in excess of 3000°C [14]. Anthracite is a hard and poorly graphitizing carbon and HTT of more than 2000°C are needed in order to obtain any significant degree of graphitization by thermal means alone.

It is, however, known that certain metals have a catalytic effect on the structural rearrangement of carbons. Some transition, alkali and alkaline earth as well as other metals from the periodic system are known to accelerate graphitization of both hard and soft carbons. It has been proposed that a metal is inactive for graphitization only if carbon has a small solubility in it, the metal carbide is extremely stable, or the metal does not wet carbon [14]. Most catalytic graphitization studies have, however, been performed above 2000°C.

The graphitization mechanism of bottom blocks at cell operating temperature is not known in detail but the action of absorbed sodium alone seems not to be able to catalytically graphitize the material [15,16]. Circumstantial evidence indicates that a carbide disproportionation or dissolution-precipitation mechanism is

Table 2. Apparent density, impurity content (ash) and X-ray diffraction parameters measured on virgin and used cathode blocks.

		Bottom Block Type A2				Bottom Block Type B3			
Age	(yrs)	0	0.4	4.4	4.6	0	4.9	6.9	7.2
Density*	(kg/m3)	1518	1626	2121	2051	1514	2212	2031	2259
Ash*	(%)	4.5	13.0	29.0	24.1	3.4	33.4	35.0	26.8
Lc	(A)	881	119	596	369	694	847	845	1935
d002	(A)	3.370	3.374	3.373	3.369	3.376	3.365	3.364	3.368
Degree of graphitization, g [12]	(%)	66	58	63	70	55	72	77	70
Peak ratio, p002 [13]	(%)	-	-	15.3	12.7	9.7	14.6	30.9	32.1
Graphite content from p002	(%)	-	-	41	34	26	39	84	87

*) Before fluoride removal.

operative, since only carbon that also have been penetrated by bath components graphitize. The transformation from disordered carbon to graphite does not take place smoothly and evenly throughout the carbon matrix but along distinct reaction boundaries [17]. The graphite formation goes probably through the carbide stage in which a carbide particle, or more probably a carbide front, moves through the carbon. Intermediate carbide species are formed in the front [18]:

$$MC_{1-x} + yC_{amorphous} = MC_{1-x+y} \quad (3)$$

that later decomposes and leaves graphite behind:

$$MC_{1-x+y} = MC_{1-x} + yC_{graphite} \quad (4)$$

The reaction can continue isothermally because of the negative free energy change in going from disordered carbon to graphite. It is reason to believe that aluminium carbide, Al_4C_3, which is formed throughout the bottom block during operation [1], is the active catalyst [19], although catalytic activity of other metal impurities in the block can not be ruled out.

Refractories and Insulation. While the major change that takes place in the carbon lining with age is a structural rearrangement, the oxide refractory and insulation layers underneath the carbon pane may be subject to extensive conversion through chemical reactions with penetrating bath or bath components. The chemical reactions that take place in these parts of the cathode have been discussed in several papers and an overview are given in Ref. [1].

Impregnation with fluorides and chemical conversion leads to a densification of the material which will affect its thermal properties. An increase in apparent density of firebricks from ≈2100 kg/m^3 to >2600 kg/m^3 is not uncommon. Open porosity may drop from >20 % to practically zero. While this may have only marginal effects on the thermal properties of dense bricks, a similar conversion and densification of the insulation layers may have a catastrophic effect on the total thermal balance and energy efficiency of the cell. The change in apparent density of these materials can be much more dramatic since they may consist of >85 % porosity.

The thermal properties of a refractory powder barrier may serve as an example. In its powdery state it is a fairly dense (≈2000 kg/m^3) and decent thermal insulator (Figure 12), although not as good as the low density vermiculite slab also shown on the figure. In its chemically converted and densified (>2700 kg/m^3) state the thermal conductivity becomes more comparable to dense refractory materials. There is, however, one important difference. Its insulating properties improve as the temperature is increased.

The negative temperature coefficient of the thermal conductivity is a consequence of the densification. The pores disappear and the mechanism of conduction changes from emission and convection in the pores to phonon conduction typical of a crystalline ionic material, see for instance Seltveit [20].

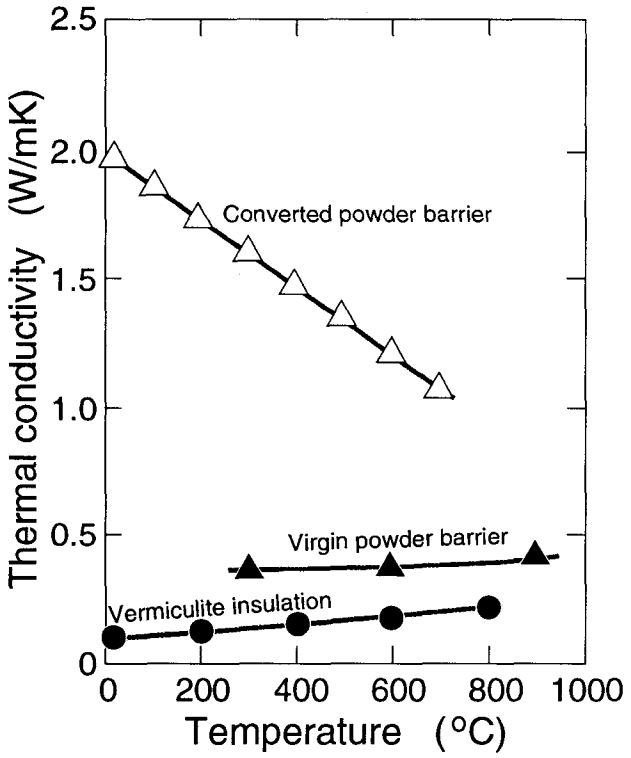

Figure 12. Thermal conductivity of virgin and converted powder refractory barrier material used in aluminium reduction cell cathodes. Data for virgin vermiculite insulation slabs are included for comparison.

Cathode Modelling. A requisite for the proper use of models to simulate industrial processes is realistic input data. This is also true with respect to design, temperature and heat balance modelling of cathodes for aluminium reduction cells. From the preceding discussion it becomes clear that the use of virgin data only for critical material parameters such as electrical and thermal properties of cathode lining materials may be of limited value.

Some results of simple thermal modelling of a cathode with virgin and aged lining materials are shown in Figure 13. Figure 13a show

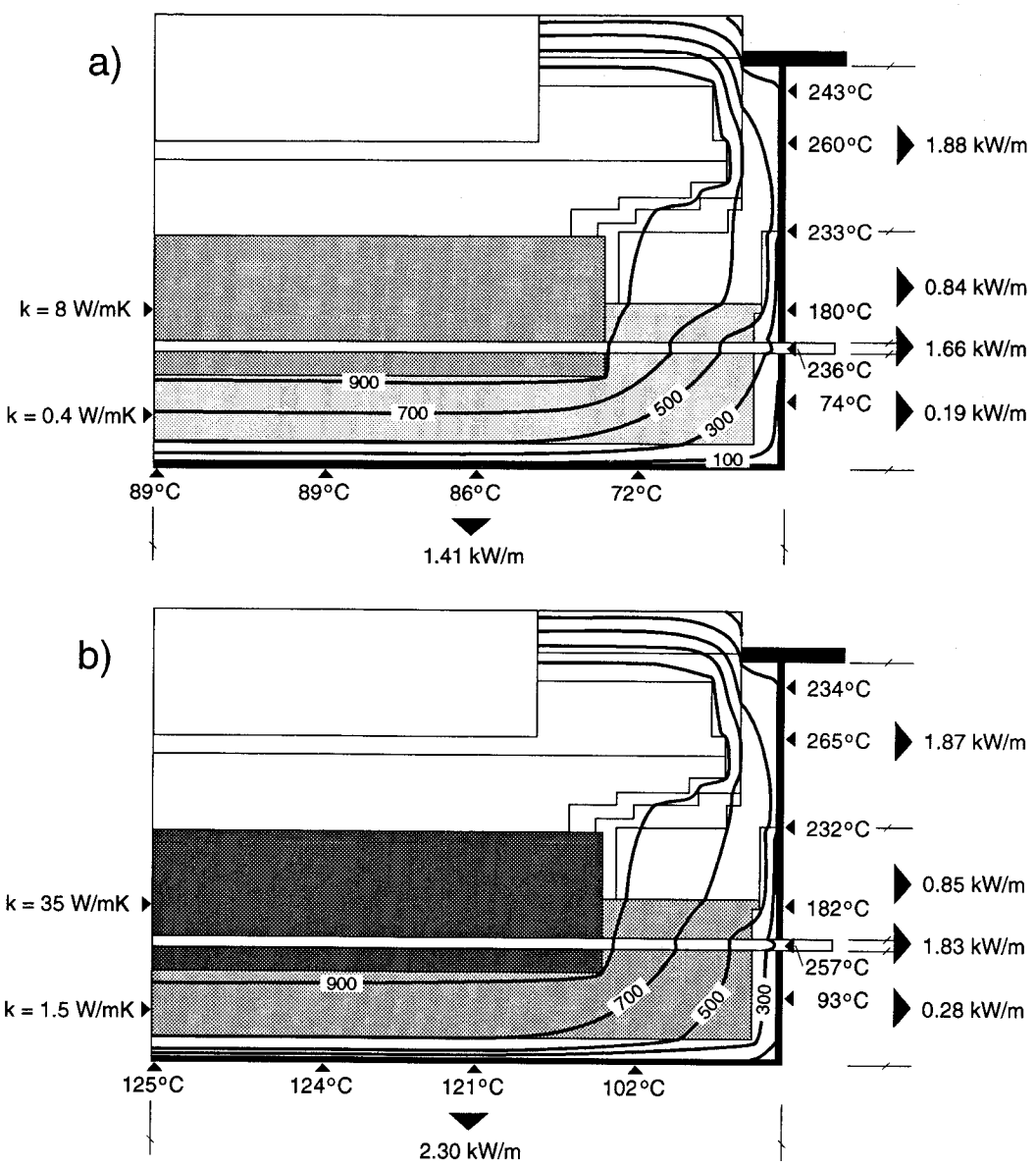

Figure 13. Thermal model calculations of an aluminium reduction cell cathode design.

a) Virgin materials only: Amorphous block, refractory powder barrier, calcium silicate back-up insulation protected by steel plate.

b) Aged and converted lining materials: Partially graphitized cathode block, converted refractory powder barrier, intact insulation next to steel shell.

the calculated isotherms and heat fluxes for a cathode with virgin lining materials consisting of amorphous bottom blocks, a refractory powder barrier and calcium silicate slabs next to the steel shell. Figure 13b shows the calculated situation after approximately 1 year in service. The bottom block is partly graphitized and the powder barrier is fully converted. The calcium silicate insulation is left intact in these calculations. The temperature changes and heat losses would have been much more pronounced if the bottom insulation layer had been attacked.

Industrial Experience of Refractory Breakdown. More dramatic changes in thermal properties may take place if the oxide refractory material, or rather its silica content, is converted with aluminium metal in an aluminothermic reaction:

$$3SiO_2(s) + 4Al(l) = 2Al_2O_3(s) + 3Si(l, diss.) \qquad (5)$$

Massive leaks of metal into porous insulation materials have resulted in aluminothermic conversion of the entire insulation bottom and a total filling of the porous structure with metal (Figure 14). During the exothermal reaction the steel shell bottom may become red-hot. Thermal conductivity of the metal-reacted insulation increased by a factor of close to 500 (Figure 15). Although such a pot could be operated for some time after such an incident, the heat losses would be vey large and a steady state steel bottom temperature of ≈400°C would lead to steel shell deformations. A simultaneous presence of a certain amount of bath or bath components is probably necessary in order to make the reaction proceed to such an extent.

Dense refractory materials may also react with metal in a similar way although the extent of reaction or conversion is normally on a smaller scale than described above. The reactions with dense materials also seem to affect the lining only locally. Metal conversion and impregnation of low porosity refractories are usually seen in the vicinity of other failures or leaks where both metal and electrolyte are readily available. Metal leaks that provide a direct collector bar-metal pad contact may result in increased temperatures locally and favourable reaction conditions. Figure 16 shows a cross-section of a refractory low cement castable (LCC) from a failed pot. The LCC was used as a barrier between the lower half of the bottom blocks and the side insulation. The part

Figure 14. A massive leak of metal into the vermiculite insulation of a cathode has converted its silica content in an aluminothermic reaction and replaced the previous porosity. The material left in the pot shell consist of the former insulation slabs, now reacted and impregnated with 8-10 tonnes of metal. Potlife was 5 days [1].

shown on the figure was close to the site of the terminal failure which happened to be a pothole through the peripheral ramming. Castable further away from the failure had not reacted this way.

Figure 17 shows the development of average bottom temperature since shortly after start-up on a group (16) of 155 kA cells with prebaked anodes. The bottom temperature increases steadily with age caused by a slow deterioration of the insulation layers. The seasonal climatic changes at the smelter site are superimposed. The average bottom temperature (t in °C) as a function of time (τ in days) is fitted to the polynom:

$$t_{aver} = 134.1 + 1.555 \cdot \sqrt{\tau} + 0.009035 \cdot \tau \quad (6)$$

with a coefficient of correlation R = 0.948.

By looking at individual cells in the population differences in the thermal insulation deterioration could be followed. Each cathode had three thermocouples welded to the bottom steel shell, one near the middle and two closer to the ends. The bottom insulation consisted of two layers of vermiculite slabs with steel plates on top of each. The steel plates served as vapour barriers and protection against bath leaks. Figure 18 shows the development in maximum bottom temperature difference on two of these pots. As long as the insulation remains intact there is practically no temperature gradient over the steel bottom. Barrier penetration by bath followed by deterioration of insulation normally starts locally. It propagates horizontally through the exposed insulation layer from the initial failure site since a back-up layer of steel plates still protects the bottom insulation layer. The measured temperature difference will thus start to increase, go through a maximum and reach zero again when the layer is fully converted.

Pot 1 in Figure 18 developed a small leak through the top steel barrier after about 6 months in service but after more than 4 years the upper insulation layer is still not fully

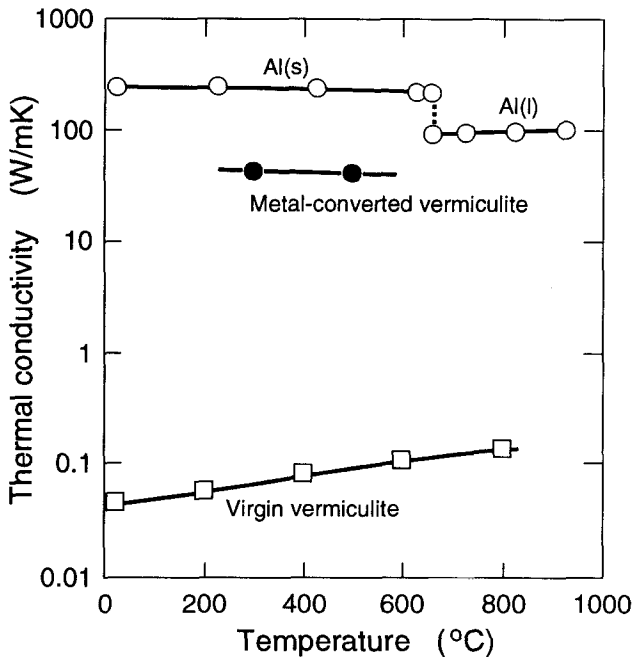

Figure 15. Thermal conductivity measured on metal-infiltrated insulation. Data for virgin insulation and aluminium metal are included for comparison [1].

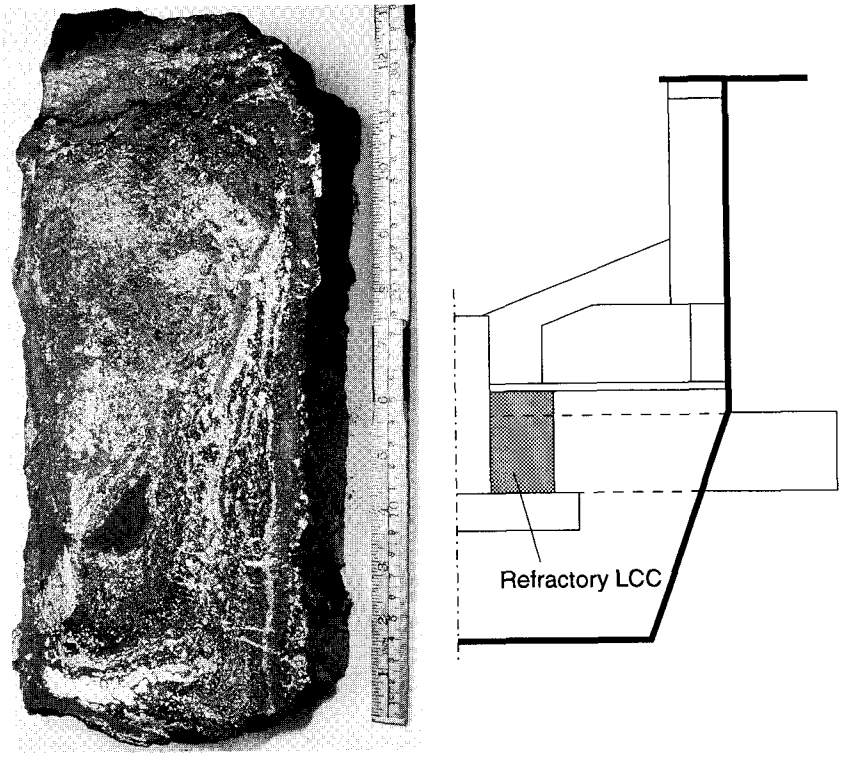

Figure 16. Cross-section of refractory LCC dam shows metal penetration and reaction. Light phase is metal but metal has also infiltrated grey areas with the exception of small dark-grey core near the middle of the lower half of the section. Potlife was 350 days [1].

converted. Pot 2, on the other hand, experienced a massive influx of bath into the upper insulation layer after start and the layer was fully converted in less than a year. After about two years bath penetrated the last protective barrier and started to attack the bottom insulation layer. The average bottom temperature was more than 40°C higher on Pot 2 than on Pot 1 at the end of the period shown on the figure.

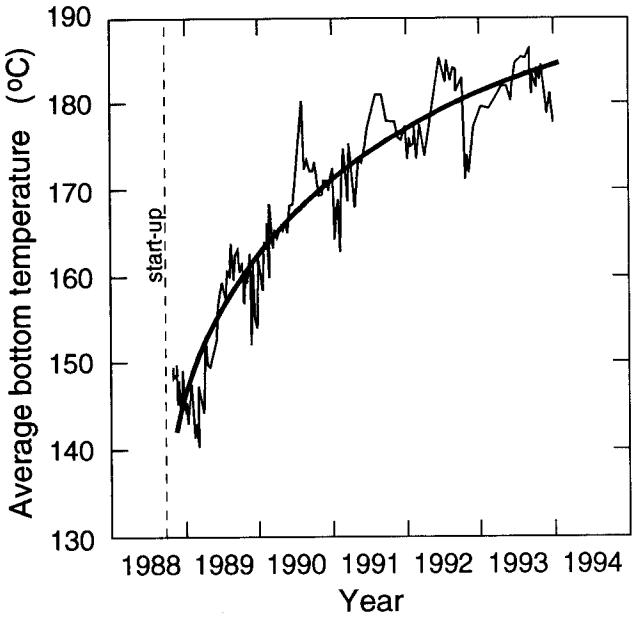

Figure 17. Development of average bottom temperature for a group of 16 cells (155 kA prebaked) since start-up. Thin curve: Measurements; Thick curve: Polynom fit.

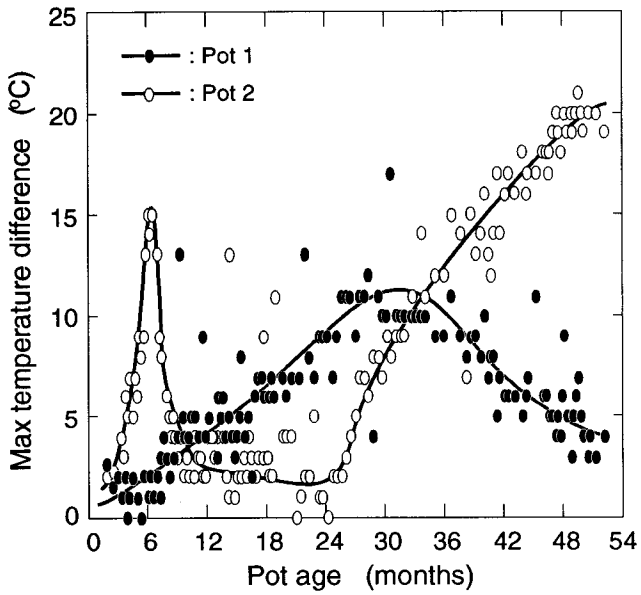

Figure 18. Maximum difference in measured steel shell bottom temperatures for two identically lined and operated pots plotted against service life [1].

CONCLUSIONS

Changes in commercial carbon cathode properties have been studied as a function of time in operation.

Anthracitic blocks are catalytically graphitized, probably with Al_4C_3 as an intermediate.

The peak ratio p_{002} of the d_{002} X-ray diffraction line characterizes the graphitization well.

Graphitization and melt penetration result in:

- Electrical resistivities of anthracitic blocks nearly equal to graphitic blocks.
- Thermal conductivities equal to or higher than graphitic blocks.

Electrical and thermal properties are not found to correlate well.

The changes in thermal conductivities of refractory and insulation materials have also been determined.

Heat balance calculations demonstrated the need to use actual values for thermal conductivity, not only those of virgin materials.

Some industrial examples of cathode refractory and insulation breakdown are given.

Acknowledgements: The authors wish to thank *Elkem Aluminium ANS* for funding the work and for permission to publish. HAØ is grateful for financial assistance from *The Research Council of Norway* through the EXPOMAT program.

REFERENCES

1. M.Sørlie and H.A.Øye, *"Cathodes in Aluminium Electrolysis, 2nd Edition"*, Aluminium Verlag, Düsseldorf, Germany, 1994.

2. P.Brilloit, L.P.Lossius, and H.A.Øye, "Melt Penetration and Chemical Reactions in Carbon Cathodes during Aluminium Electrolysis. I. Laboratory Experiments", *Light Metals* (1993) 321 (corrected version in *Light Metals* (1994) 1237).

3. L.P.Lossius and H.A.Øye, "Melt Penetration and Chemical Reactions in Carbon Cathodes during Aluminium Electrolysis. II. Industrial Cathodes", *Light Metals* (1993) 331.

4. R.Shamsili and H.A.Øye, "Melt Penetration and Chemical Reactions in Carbon Cathodes during Aluminium Electrolysis III", *Light Metals* (1994) 731.

5. O.-J.Siljan, C.Schøning, and A.Seltveit, "Investigations of Deteriorated Alumina Reduction Pot Lining", UNITECR, Aachen, Germany (1991) 31.

6. O.-J.Siljan, Sodium Aluminium Fluoride Attack on Alumino-Silicate Refractories", Dr.ing. Thesis, Institute of Inorganic Chemistry, The Norwegian Institute of Technology, Trondheim, Norway, 1990.

7. F.Brunk, W.Becker, and K.Lepère, "Cryolite Influence on Refractory Bricks. Influence of SiO_2 Content and Furnace Atmosphere", Light Metals (1993) 315.

8. F.Brunk, "Corrosion and Behaviour of Fireclay Bricks of Varying Chemical Composition Used in the Bottom Lining of Reduction Cells", Light Metals (1994) 477.

9. W.Haupin, "Cathode Voltage Loss in Aluminium Smelting Cells", *Light Metals* (1975) 339.

10. M.Sørlie and H.Gran, "Cathode Collector Bar-to-Carbon Contact Resistance", *Light Metals* (1992) 779.

11. T.Log and H. A.Øye, "A New Transient Hot-Strip Method for Determination of Thermal Conductivity of Carbon Materials up to 700°C", *Light Metals* (1990) 473.

12. J.Maire and J.Méring, "Graphitization of Soft Carbons", in *Chemistry and Physics of Carbon, Vol. 6*, ed. P.L.Walker, Jr. and P.A.Thrower, Marcel Dekker, Inc., New York, NY, 1970, p.125.

13. F.Aune, W.Brockner and H.A.Øye, "X-Ray Characterization of Cathode Carbon Materials", *Carbon* **30** (1992) 1001.

14. W.L.Holstein, R.D.Moorehead, H.Poppa, and M.Boudart, "The Palladium-Catalyzed Conversion of Amorphous to Graphitic Carbon", in *Chemistry and Physics of Carbon, Vol. 18*, ed. P.A.Thrower, Marcel Dekker, Inc., New York, NY, 1982, p.139 (and references therein).

15. M.Sørlie and H.A.Øye, "Chemical Resistance of Cathode Carbon Materials during Electrolysis", *Light Metals* (1984) 1059.

16. J.Waddington, "Processes Occuring in the Carbon Lining of an Aluminum Reduction Cell", in *Extractive Metallurgy of Aluminum, Vol. 2*, ed. G.Gerard, Interscience Publishers, New York, NY, 1963, p. 435.

17. N.W.Muller and F.L.Shea, Jr., "An Investigation of Aluminum Cell Cathode Liners and Materials", in *Extractive Metallurgy of Aluminum, Vol. 2*, ed. G.Gerard, Interscience Publishers, New York, NY, 1963, p. 417.

18. A.Oya and H.Marsh, "Phenomena of Catalytic Graphitization", *J.Materials Science* **17** (1982) 309.

19. A.Oya and S.Otani, "The Effects of Aluminum on Structural Development of a Carbon Derived from Phenolic Resin", *Carbon* **14** (1976) 191.

20. A.Seltveit, *Ildfaste Materialer*, Tapir, Trondheim, Norway, 1992.